

from the chamber wall and may thus provide better flame stability. No near-wall recirculation zone is generated, thus the hot spot problem can be alleviated.

In the present study, pressure loss is expressed in terms of a stagnation pressure recovery coefficient defined as the ratio of the mass-averaged stagnation pressure at the end of the combustion chamber to the stagnation pressure at the entrance of the side inlets. The recovery coefficient for the original DSIC configuration was found to be 0.96, whereas that of the DSIC with the cone swirler configuration is about 0.79. This pressure loss is acceptable, considering the improvement in fuel/air mixing with improved flow patterns and stronger flow swirl. This pressure loss undoubtedly can be improved as the swirler geometry is optimized.

Flow swirl was quantified as swirl intensity (S.I.), defined as the mass-averaged ratio of tangential kinetic energy to the total kinetic energy. The S.I. is almost zero for the original DSIC design, except near the dome region, because mixing in the DSIC is only significant in the shear layers between the incoming airstreams and the surrounding air. For the DSIC with a cone swirler the S.I. is larger than 0.3 throughout the combustion chamber, which is a significant improvement on the original DSIC configuration.

Summary

A feasible cone swirler design for a side-inlet ducted ram-rocket combustor has been demonstrated and its advantages illustrated using the KIVA3 program. Studies of the nonreacting flowfield indicate that the cone swirler not only improves the flow pattern, but also enhances the flow swirl in the combustor. Use of the cone swirler should result in better fuel/air mixing and more complete combustion in the combustion chamber, without significant pressure losses. The primary recirculation zone is generated by vortex breakdown and is located at the combustor center; it can be used as an aerodynamic flameholder to stabilize the reacting field. It is thus anticipated that the DSIC with a cone swirler will be more efficient than the DSIC without a swirler. The swirler concept is general and can be applied to combustors with different geometries. To quantify the effects of pressure losses on missile thrust, however, reacting flows must be studied.

Acknowledgments

This study was supported by and performed at Wright-Patterson Air Force Base, under Contract F33615-94-C-2439. Additional support was a grant of CRAY computer time from the Department of Defense CEWES High Performance Computing Center. The authors would like to thank A. A. Amsden of the Los Alamos National Laboratory for many valuable comments about the KIVA3 program, and A. E. S. Creese of Taitech, Inc., for editorial comments concerning this article.

References

- ¹Timnat, Y. M., "Recent Developments in Ramjets, Ducted Rockets and Scramjets," *Progress in Aerospace Science*, Vol. 27, No. 3, 1990, pp. 201-235.
- ²Slagle, D. R., and Braendlein, R. K., "Variable Flow Ducted Rocket (VFDR) Program," Air Force Wright Aeronautical Labs., TR-82-2130, Wright-Patterson AFB, OH, Jan. 1983.
- ³Stull, F. D., Craig, R. R., Streby, G. D., and Vanka, S. P., "Investigation of a Dual Inlet Side Dump Combustor Using Liquid Fuel Injection," *Journal of Propulsion and Power*, Vol. 1, No. 1, 1985, pp. 83-88.
- ⁴Vanka, S. P., Craig, R. R., and Stull, F. D., "Mixing, Chemical Reaction, and Flowfield Development in Ducted Rockets," *Journal of Propulsion and Power*, Vol. 2, No. 4, 1986, pp. 331-338.
- ⁵Amsden, A. A., "KIVA-3: A KIVA Program with Block-Structured Mesh for Complex Geometries," Los Alamos National Lab., Rept. LA-12503-MS, March 1993.
- ⁶Liou, T.-M., and Wu, S.-M., "Flowfield in a Dual-Inlet Side-Dump Combustor," *Journal of Propulsion and Power*, Vol. 4, No. 1, 1988, pp. 53-60.

⁷Escudier, M. P., and Keller, J. J., "Recirculation in Swirling Flow: A Manifestation of Vortex Breakdown," *AIAA Journal*, Vol. 23, No. 1, 1985, pp. 111-116.

Payload to Low Earth Orbit by Aerospace Plane with Scramjet Engine

Takeshi Kanda* and Kenji Kudo†
National Aerospace Laboratory,
Kimigaya, Kukuda, Miyasi 981-15, Japan

Introduction

Aerospace plane is being studied as the new transportation system to low earth orbit (LEO). The propulsion system of the aerospace plane requires several engines: an air-turbo-ramjet engine (ATR), a scramjet engine, and a rocket engine.

In the present research, the characteristics and role of the scramjet for the single-stage aerospace plane were investigated for a LEO of 100 km. The scramjet engine is usually fueled by hydrogen, although there are several studies on the hydrocarbon-fueled scramjet engines.^{1,2} Therefore, the possibility of using methane as well as hydrogen was investigated, and the size of the payload that could be carried by various combinations of the engines was estimated.

Calculation Procedure

Flight Simulation

The aerospace plane was treated as a material point. The motion of the aerospace plane was within the horizontal and vertical plane. The schematic diagram of the forces is shown in Fig. 1, and the equations used in the study are given as follows:

$$\frac{dx}{dt} = \frac{R}{R+z} \cdot v \cdot \cos \gamma \quad (1)$$

$$\frac{dz}{dt} = v \cdot \sin \gamma \quad (2)$$

$$\frac{dv}{dt} = \frac{F \cdot \cos \delta - D}{m} - g \sin \gamma \quad (3)$$

$$\frac{d\gamma}{dt} = \frac{F \cdot \sin \delta + L}{m \cdot v} - \frac{g \cdot \cos \gamma}{v} + \frac{v \cdot \cos \gamma}{R+z} \quad (4)$$

$$\frac{dm}{dt} = -\frac{F}{I_{sp}} \quad (5)$$

In the equations, x , t , R , z , v , and γ are distance on the Earth surface, time, the radius of the Earth, height, velocity, and angle of inclination, respectively. F , δ , D , m , and g are force, angle between the engine thrust and the airframe velocity,

Received July 31, 1995; revision received July 18, 1996; accepted for publication Aug. 2, 1996. Copyright © 1996 by the American Institute of Aeronautics and Astronautics, Inc. All rights reserved.

*Senior Researcher, Ramjet Propulsion Research Division, Kakuda Research Center. Member AIAA.

†Senior Researcher, Ramjet Propulsion Research Division, Kakuda Research Center.

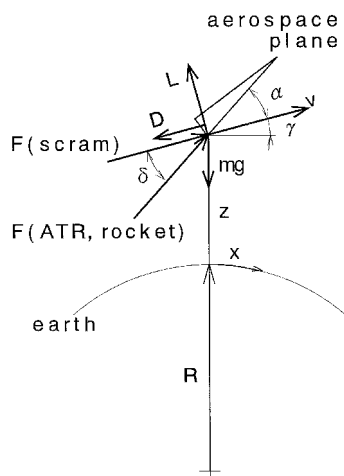


Fig. 1 Forces, velocity, and coordinates on aerospace plane.

drag, mass, and acceleration of gravity at the height of z , respectively. L and I_{sp} are lift and specific impulse defined in SI units. In Fig. 1, α is the angle of attack.

Four missions were investigated, i.e., 1) ATR \rightarrow hydrogen-fueled scramjet \rightarrow rocket, 2) ATR \rightarrow methane-fueled scramjet \rightarrow rocket, 3) ATR \rightarrow rocket, and 4) rocket \rightarrow hydrogen-fueled scramjet \rightarrow rocket. The flight dynamic pressure was equal to 100 kPa during the operation of ATR or the scramjet, except at the takeoff. The maximum acceleration was $19.6 \text{ m} \cdot \text{s}^{-2}$.

Airframe

The configuration of the aerospace plane was from Ref. 3. The body length was 77 m, the body width was 14 m, and the span was 35 m. There were six ATR modules, and six scramjet modules on the airframe. The total projected cross section of the ATR modules was 15 m^2 , whereas that of the scramjet modules was 36 m^2 . The drag of the scramjet was included in the net thrust in the scramjet operating condition and was assumed negligible in the nonoperating condition.

The initial mass was 460 ton at the horizontal takeoff. The aerospace plane was constructed from the propellants, propellant tankage, payload, engines, and airframe. The airframe was expected to become light with the advance of technology. Therefore, 50% of the estimated mass of 102.2 ton⁴ was adopted for the mass of the airframe in this study. While the mass of ATR was estimated to be 7% of the initial mass,⁴ it was set to 6% with the expected advance of technology. The mass of the scramjet was twice that of the ramjet⁴ because of the low-thrust density of the scramjet. The mass of the rocket engine was 0.7% of the initial mass.⁴

The volume of the propellant tank corresponded to the consumed liquefied propellants. The volume difference of the tank in the various missions had an influence only on the mass of the tank, and it had no influence on the dimension of the airframe. The mass of the fuel tankage was proportional to the volume of the fuel tank, and the unit mass of the tankage per unit volume of the fuel did not depend on the kind of the fuel, i.e., hydrogen or methane. The mass of the tank was also calculated according to Ref. 4.

Engines

ATR,⁵ the scramjet,⁶ and the liquid rocket engine⁷ were used for the propulsion system of the aerospace plane. ATR used hydrogen as fuel. The equivalence ratio of ATR was unity. ATR operated from the flight Mach number of 0 to 6.

The scramjet operated from Mach number 6. The cooling system of the scramjet consisted of a combination of regenerative cooling and film cooling, which will decrease the cooling requirement, and will aid maintaining adequate specific impulse.⁶

The performance of the methane-fueled scramjet was calculated in the same manner as the hydrogen-fueled scramjet.⁶ Methane was supplied at a pressure of 10 MPa and temperature of 120 K at the entrance of the engine-cooling jacket. The temperature, 120 K, was almost the boiling condition under 1 atm.

Three rocket engines were used. Liquid hydrogen and liquid oxygen with the mixture ratio of $O/F = 6$ were used as propellants. The maximum total thrust was 4057 kN, and the specific impulse was $4018 \text{ m} \cdot \text{s}^{-1}$.

Results and Discussion

Performances of the Methane-Fueled Scramjet

The specific impulse and the equivalence ratio are shown in Fig. 2. The equivalence ratio was larger than that of the hydrogen-fueled scramjet because of the low cooling capacity. There were two reasons for the low specific impulse of the methane-fueled scramjet.

1) The specific impulse increases with the heat release of the fuel and decreases with the fuel mass flow rate. At the stoichiometric condition, the heat release of methane is almost equal to that of hydrogen for a certain flow rate of the air, whereas the mass flow rate of methane is twice that of hydrogen.

2) As shown in Fig. 1, the equivalence ratio of the methane-fueled scramjet was larger than unity because of the cooling requirement.

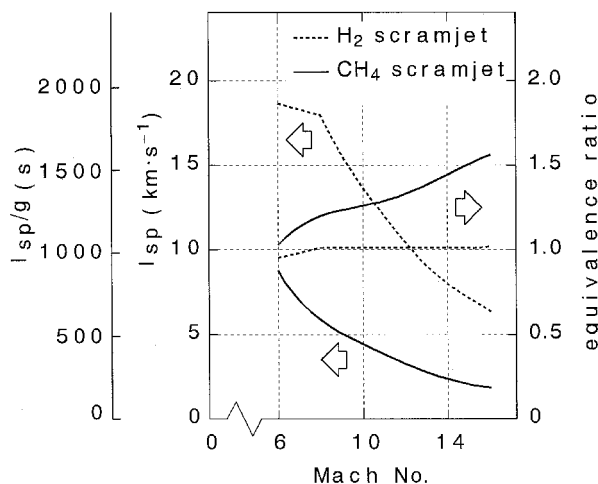


Fig. 2 Specific impulses and equivalence ratios of H_2/CH_4 scramjet engines.

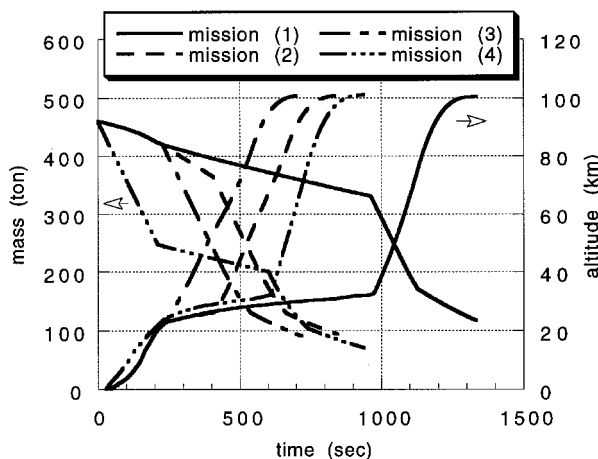


Fig. 3 Flight condition of each mission.

Table 1 Contents of mass (ton)

| Items | Mission | | | |
|----------------------|---------|-------|-------|-------|
| | (1) | (2) | (3) | (4) |
| Propellant | | | | |
| Fuel (ATR) | 40.0 | 40.0 | 40.0 | — |
| Fuel (scramjet) | 89.1 | 55.6 | — | 46.9 |
| Fuel (rocket) | 30.6 | 38.7 | 47.0 | 48.9 |
| Oxygen | 183.4 | 232.0 | 282.3 | 293.1 |
| Total propellant | 343.1 | 366.3 | 369.0 | 388.9 |
| Tank | | | | |
| H ₂ | 17.9 | 9.0 | 9.9 | 10.8 |
| O ₂ | 3.1 | 3.9 | 4.6 | 4.8 |
| CH ₄ | — | 1.4 | — | — |
| Total tank | 21.0 | 14.3 | 14.5 | 15.6 |
| Airframe and engines | 91.1 | 91.1 | 81.9 | 63.5 |
| Payload | 4.8 | —11.7 | —5.4 | —8.0 |
| Total initial mass | 460.0 | 460.0 | 460.0 | 460.0 |

Payload Estimation

In missions (1), (2), and (4) (Fig. 3), the effective operation range of the scramjet was determined to maximize the payload. The hydrogen-fueled scramjet was used up to Mach number 12 in missions (1) and (4), whereas the methane-fueled scramjet operated up to Mach number 8 in mission (2).

The velocity increment ΔV was shown as follows:

$$\Delta V = \bar{I}_{sp} \cdot [1 - (\bar{D}/\bar{F})] \cdot \ell n(m_i/m_f) \quad (6)$$

\bar{I}_{sp} , \bar{D} , \bar{F} , and m_f are mean specific impulse, mean drag, mean thrust, and final mass, respectively. The expected merit of use of the dense fuel is a result of 1) increasing the initial mass m_i , and 2) increasing the thrust, as well as 3) reducing the tank volume. The simulated results are shown in Table 1. The flight condition of each mission is shown in Fig. 3.

The payload of mission (3) with ATR was larger than that of mission (4) without ATR. The payload of mission (1) with the hydrogen-fueled scramjet was larger than that of mission (3) without the hydrogen-fueled scramjet. The most favorable operating condition for the air-breathing engine is in the low-speed range with dense air, and so the usage of ATR seems natural for the aerospace plane, and the use of the scramjet seems necessary to realize the mission to LEO by the single-stage aerospace plane.

The payload with the methane-fueled scramjet was the smallest in the missions for the following reasons:

1) In the study of the aerospace plane with horizontal take-off, the initial mass should be set the same among all of the missions, because the heavy initial mass needs the heavy landing gear and airframe.

2) The increase of the thrust caused by the usage of the methane was not realized, because the thrust of the methane-

fueled scramjet was almost the same as that of the hydrogen-fueled scramjet. This was because the working fluid of the scramjet was nitrogen, and the fuel was only the heat source, unlike in the rocket engine.

3) Though the decrease of the mass of the tank was realized in the mission with the methane-fueled scramjet, the methane-fueled scramjet had very low specific impulse, and the rocket began to be used much earlier in the mission than with the hydrogen-fueled scramjet. Therefore, the mass of the oxygen became larger.

Conclusions

The payload to LEO by the single-stage aerospace plane with the scramjet engine was estimated in the various missions. The following conclusions can be drawn:

1) The aerospace plane will need the hydrogen-fueled scramjet to realize the mission to LEO.

2) Methane was not suitable as fuel for the scramjet.

3) The effective operation of the scramjet was up to flight Mach number 12.

Acknowledgments

The authors thank Goro Masuya of Tohoku University, and Nobuo Chinzei and Yoshio Wakamatsu of the National Aerospace Laboratory for discussions.

References

- ¹Chiniz, W., and Holgeson, J., "A Performance Assessment of Hydrocarbon Scramjet Engines Using a Generalized Analysis Code," AIAA Paper 95-2768, July 1995.
- ²Solomon, W., and Davis, K., "Consideration of Methane as a Fuel for an Engine in a Hypersonic Vehicle," AIAA Paper 95-2769, July 1995.
- ³Nomura, S., Hozumi, K., Kawamoto, I., and Miyamoto, Y., "Experimental Studies on Aerodynamic Characteristics of SSTO Vehicle at Subsonic to Hypersonic Speeds," *Proceedings of the 16th International Symposium on Space Technology and Science*, Committee of International Symposium on Space Technology and Science, Sapporo, Japan, 1988, pp. 1547-1554.
- ⁴Glatt, C. R., "WAATS—A Computer Program for Weights Analysis of Advanced Transportation Systems," NASA CR-2420, Sept. 1974.
- ⁵Sakata, K., Yanagi, R., Shindo, S., Minoda, M., and Nouse, H., "Conceptual Study on Air-Breathing Propulsion for Space Plane," *Proceedings of the 16th International Symposium on Space Technology and Science*, Committee of International Symposium on Space Technology and Science, Sapporo, Japan, 1988, pp. 107-112.
- ⁶Kanda, T., Masuya, G., Ono, F., and Wakamatsu, Y., "Effect of Film Cooling/Regenerative Cooling on Scramjet Engine Performances," *Journal of Propulsion and Power*, Vol. 10, No. 5, 1994, pp. 618-624.
- ⁷Kanmuri, A., Kanda, T., Wakamatsu, Y., Torii, Y., Kagawa, E., and Hasegawa, K., "Transient Analysis of LOX/LH₂ Rocket Engine (LE-7)," AIAA Paper 89-2736, July 1989.